

Communication

Correlation Between the Microstructural Development of Bainitic Ferrite and the Characteristics of Martensite-Austenite Constituent

HIDENORI TERASAKI and YU-ICHI KOMIZO

Microstructural development of bainitic ferrite under a simulated weld heat-affected zone (HAZ) of low-carbon steel was correlated with the characteristics of martensite-austenite (M-A) constituent. By combining laser scanning confocal microscopy (LSCM) observations and electron backscatter diffraction (EBSD) analysis, we evaluated variant pair formation in time-series, which was related to the second-phase formation phenomenon. Furthermore, the classification of the microstructural development showed that the characteristics of M-A in a weld HAZ can be predicted from the microstructural development of bainitic ferrite.

DOI: 10.1007/s11661-013-1998-y

© The Minerals, Metals & Materials Society and ASM International 2013

Martensite-austenite (M-A) constituents are detrimental for the toughness properties in the heat-affected zone (HAZ) or in intercritically coarse-grained HAZ (ICCGHAZ) of high-strength low-alloy steel welds.^[1-5] M-A itself acts as a microcrack or is debonded from the matrix, which results in microcracks at the interface. M-A is the second phase formed with bainitic ferrite during the microstructural development under the thermal cycle of welding. Consequently, understanding the microstructural development of bainitic ferrite is important and should be related to the characteristics of the formed M-A.

Numerous studies elucidated the microstructural characteristics of bainitic ferrite from the viewpoints of morphology and crystallography.^[6-9] Furuhashi *et al.*^[6,7] showed the effect of the driving force on the crystallographic characteristics of bainitic ferrite in Fe-Ni-C alloys under isothermal transformation conditions. At higher transformation temperatures (*i.e.*, under a weak driving force), laths of two or three variants (V1-V4-V8) with small misorientations often dominate the bainite microstructure. Takayama *et al.*,^[9] who used statistical evidence of the variant pair fraction, reported the same tendency in low-carbon steel. With respect to the

morphology and characteristics of M-A in low-carbon steel under continuous cooling conditions, Lambert *et al.*^[10] showed that small M-A's are formed at high cooling rates along the simulated cycle of the CGHAZ. In ICCGHAZ, blocky M-A is formed at the prior austenite grain boundary (PAGB) and elongated M-A is formed inside the grains. When the cooling rate is slow, granular bainite and isolated austenite (not mixed M-A) are formed. However, few studies focused on the correlation of M-A formation with the microstructural development of bainitic ferrite are reported in the literature.

In a previous study,^[11] using high-magnification orientation image maps, we showed the relationship between the misorientation of bainitic ferrite and the characteristics of the M-A constituents. We found that if bainitic ferrite has numerous low-angle boundaries, then a blocky-type retained austenite (referred to as "isolated austenite" by Lambert *et al.*^[10]) is observed and is not stable (it often contains martensite). This type of austenite development is referred to as "type A." However, if bainitic ferrite has few low-angle boundaries, then the retained austenite exhibits a rod-type shape and is stable. This type of austenite development is referred to as "type B." However, the classification criterion is only the amount of low-angle boundaries and is not enough.

In the present work, variant pair analysis of bainitic ferrite in the cases of types A and B is presented by combining with the time-series analysis of microstructural development, and it is related to the characteristics of the M-A constituents. Furthermore, on the basis of these findings (*i.e.*, the relationship between the microstructural development of bainitic ferrite and the characteristics of the M-A constituents), we try to predict the M-A morphology and stability of austenite from the microstructural development of bainitic ferrite observed by laser scanning microscopy.

A low-carbon steel with a composition of Fe-0.1C-1.0Ni-0.8Mn-0.4Mo-0.04V (mass pct) was used. The specimens were austenitized at 1623 K (1350 °C) for 30 seconds and were then cooled at 1.67 K/s to room temperature, which simulated a weld HAZ with a large heat input. Microstructural development under the thermal cycle was observed *in situ* using laser scanning confocal microscopy (LSCM) for high-temperature applications. The details of the system are described elsewhere.^[11,12] Electron backscatter diffraction (EBSD) measurements were performed in a scanning electron microscope equipped with an EBSD system operated at an acceleration voltage of 15 keV and with step sizes of 0.2 and 0.05 μm . A procedure of grain dilation cleanup was performed on the as-acquired dataset. Furthermore, points with a low confidence index (less than 0.1) were excluded to ensure the reliability of determination of phase.^[13]

The variant pair was determined using Kurdjumov-Sachs orientation relationship (KS OR), and the misorientation data between variants are reported elsewhere.^[9,14] By combining the LSCM observations and EBSD analysis, we evaluated variant pair formation in time-series, which was related to the second-phase formation phenomenon. The analyzed targets were the transformation products from a large prior austenite

HIDENORI TERASAKI, Associate Professor, and YU-ICHI KOMIZO, Professor, are with the Joining and Welding Research Institute, Osaka University, Osaka 567-0047, Japan. Contact e-mail: hidenori@jwri.osaka-u.ac.jp

Manuscript submitted May 10, 2013.

Article published online October 1, 2013

grain shown in our previous article,^[11] and new transformation products formed in the present study; our objective was to predict the position, morphology, and stability of the second phase.

Figure 1(a) shows the α -orientation map transformed from a single large prior austenite grain. A part of the α -orientation map is classified as “type A” (block (i) in Reference 11) and “type B” (block (ii) in Reference 11) from the viewpoint of amount of low-angle boundaries, as discussed previously. In type A, the variant pairs in KS OR are analyzed and marked on each orientation. The variant 1, 4, and 8 (V1-V4-V8) pair is observed, and the variants are separated by a low-angle boundary, as shown in Figure 1(b). The misorientation angle between 4.0 and 15.0 deg is defined as a low-angle boundary in Figures 1(b) and (c). The rotation axis and angle between the V1 and V4 pair are [011] and 10.53 deg, respectively. In the case of the V1-V8 pair, the axis and angle are^[1-11] and 10.53 deg, respectively.^[14] These variants belong to the same Bain group. In addition, we confirmed that the determined V1-V4 belongs to the same close-packed (CP) planes group and that the V1-V8 belongs to a different CP group. The second phase (blocky retained austenite and M-A) can be observed along or close to the V1-V4-V8 (same Bain group and different CP group) boundaries, as shown in Figure 1(b). However, in type B, a single variant was developed by thickening, as shown in Figure 1(c). An elongated second phase is distributed between the bainitic ferrite laths.

From the viewpoint of variant pairs and microstructural development along a simulated thermal cycle of the HAZ, the behaviors of types A and B are summarized in Figure 2. The characteristics of type A based on the results of the LSCM images shown in Figures 2(b) through (d) and the crystallographic analysis in Figures 1(a) and (b) are summarized in Figure 2(a). At a higher temperature (822 K (549 °C) in Figure 2(b)), V1 is formed closely parallel to the PAGB, as shown in Figure 2(c). When the temperature was decreased (764 K (491 °C) in Figure 2(d)), V4 or V8 formed, as shown in Figures 2(d) and 1(a). These variants have low-angle boundaries against V1. Along or close to the low-angle boundaries, a blocky M-A is formed. In this blocky-type M-A, the austenite exhibits low stability, as shown in our previous study.^[11] Our observation elucidated that the V1, V4, and V8 did not form at the same time. The transformation temperature difference between V1 and V4 or V8 induced the space and concentration of carbon between these boundaries and resulted in blocky M-A distributions.

In contrast, in type B, V1 is formed and the growth direction has a high angle against the PAGB, as shown in Figure 2(f). After the formation of V1, the microstructure develops *via* thickening of the single variant, as shown in Figures 2(g) and (h). The elongated M-A is formed within the thickened bainitic ferrite, and its distribution is more homogenous than that in type A. The austenite in the elongated M-A is highly stable, as shown in Reference 11. These results are summarized in the schematic illustration in Figure 2(e). These

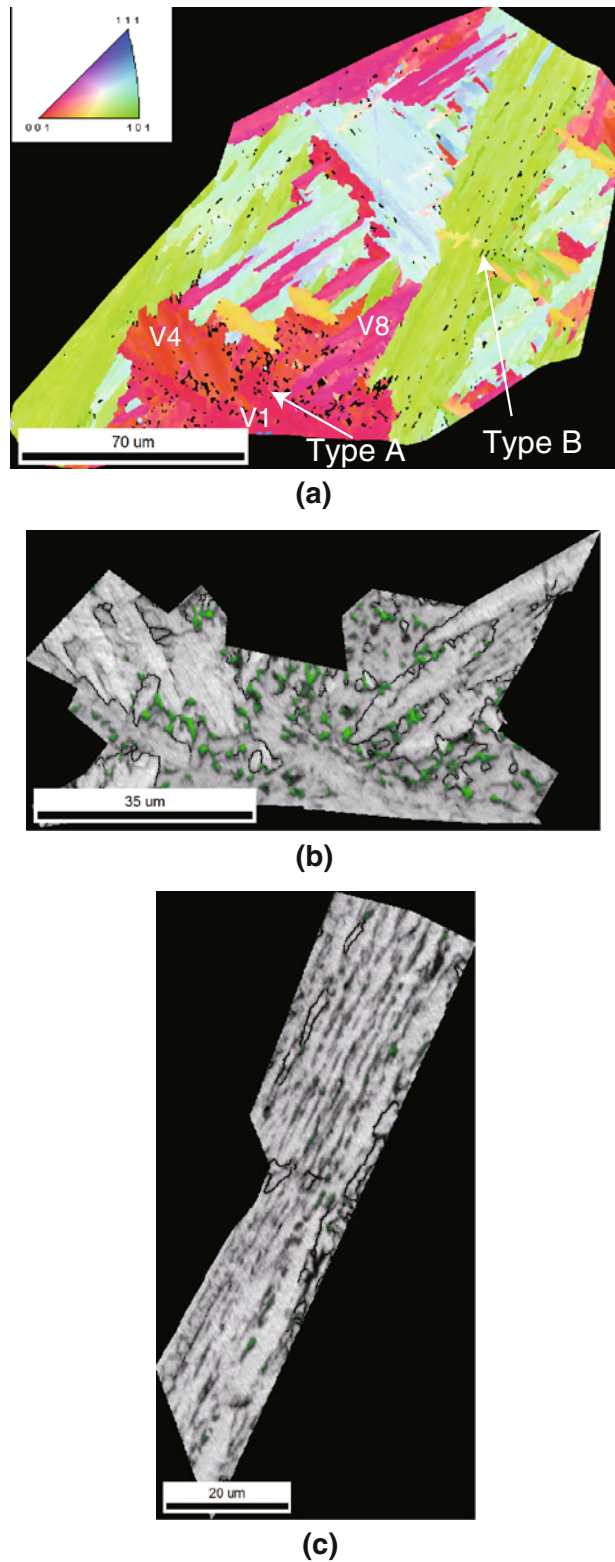


Fig. 1— α -Orientation map transformed from a single large prior austenite grain: (a) α -orientation map showing types A and B. Variants were determined using KS OR in the type A area. Image quality map of (b) type A area and (c) type B area superimposed with the phase map for austenite (green color) and low-angle boundaries (black line).

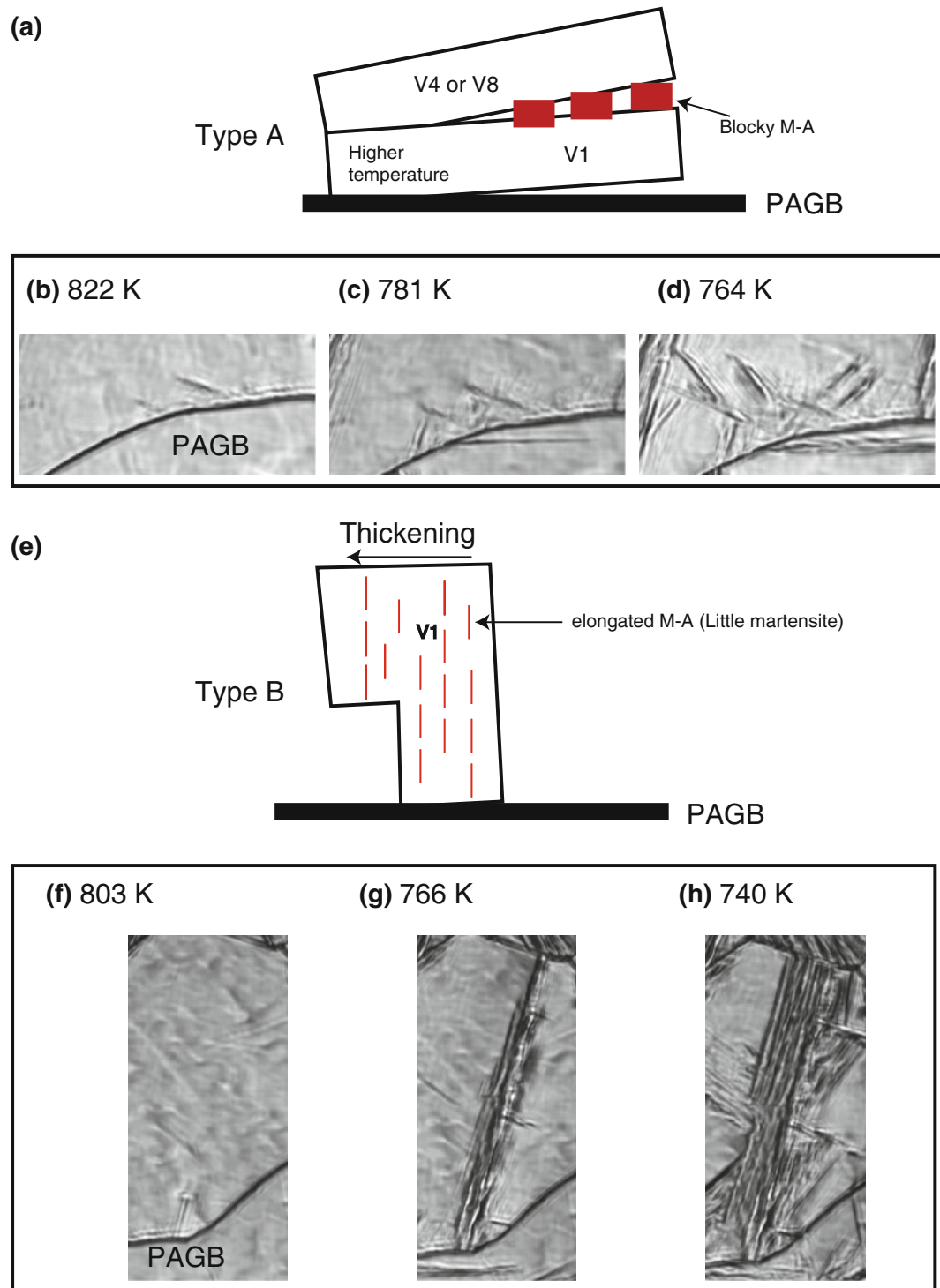
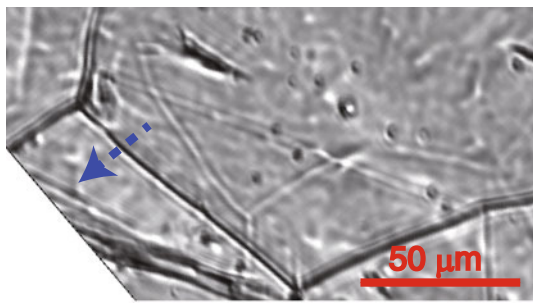


Fig. 2—Schematic illustrations of the microstructural development of bainitic ferrite and M-A: (a) type A and (e) type B. The LSCM images corresponding to (b) through (d) type A and (f) through (h) type B are also shown for each type.

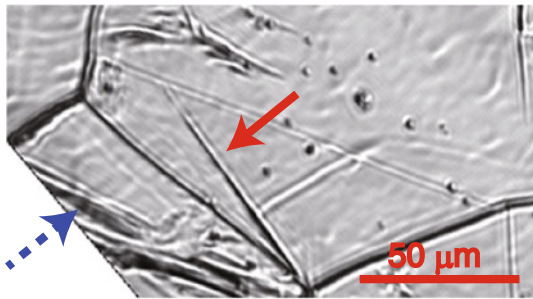
classifications suggest that the characteristics of M-A (e.g., the morphology, stability of austenite, and location of where it is distributed) can be predicted when the microstructural development is observed.

To confirm type classification shown in Figure 2, we performed new observations of microstructural development using steel with the same chemical composition and

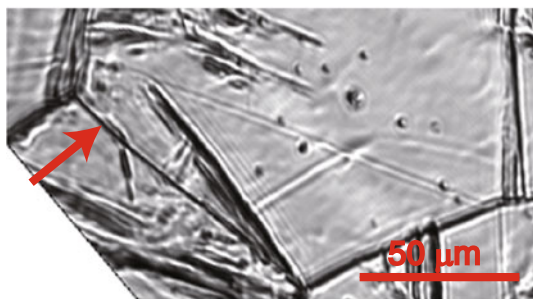
under the same thermal cycling conditions. Figure 3 shows the microstructural development observed using LSCM. At 820 K (547 °C), bainitic ferrite nucleates and grows with a high angle against the PAGB. After that, the microstructure develops *via* thickening, as shown in Figures 3(a) and (b), indicated by blue arrows. This type of microstructural development is predicted to be type B



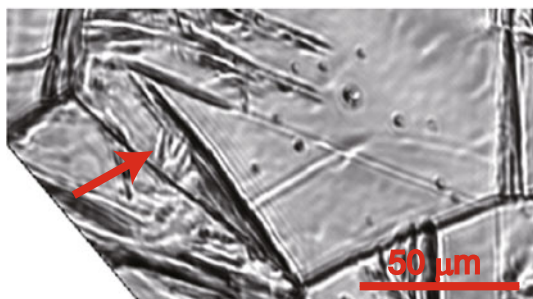
(a) 820 K



(b) 807 K



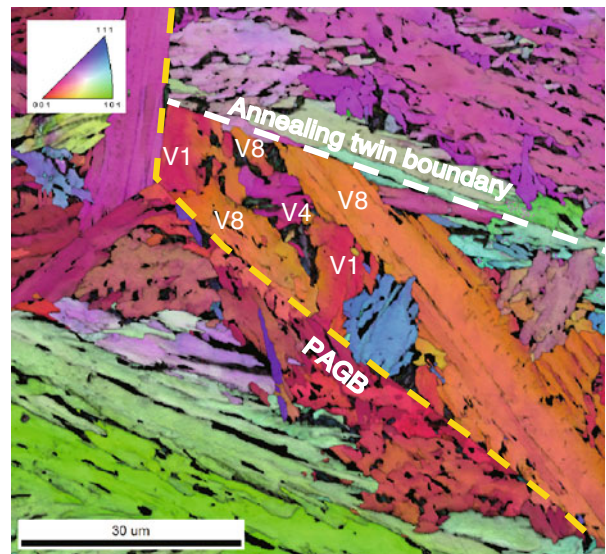
(c) 789 K



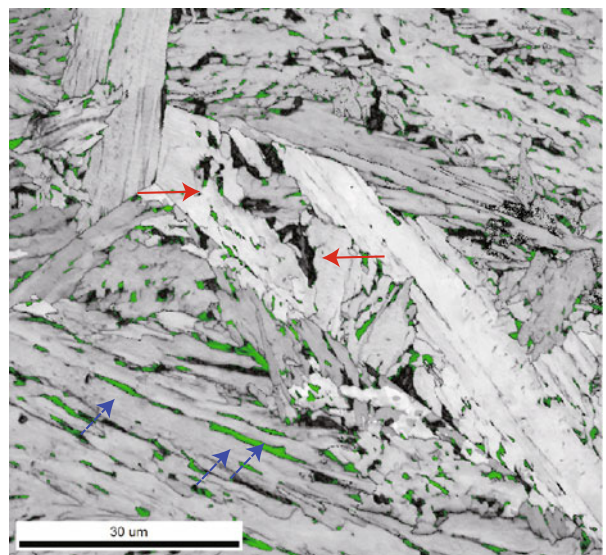
(d) 784 K

Fig. 3—(a) through (d) LSCM images of the microstructural development of bainitic ferrite for a new grain. Bainitic ferrite indicated by blue arrows in (a) and (b) are typical characteristics of the microstructural development in type B. Bainitic ferrite indicated by red arrows in (b) through (d) are typical characteristics of the microstructural development in type A.

and elongated M-A is expected to form. As shown in Figure 3(b), other bainitic ferrite nucleates and grows with a small angle against the PAGB (807 K (534 °C)), indicated by red arrows. In addition to the PAGB, a transparent boundary was observed within the austenite,



(a)



(b)

Fig. 4—Orientation analysis of bainitic ferrite and the second phase corresponding to the microstructure shown in Fig. 3: (a) α -orientation map (superimposed with the image quality map) and analyzed variant pair and (b) image quality map superimposed with the phase map for austenite (green color). The red arrows show retained austenite in type A mode and the blue show that in type B mode.

which we estimated to be a twin boundary. The growth of bainitic ferrite stopped at the transparent boundary. As the temperature decreased, different bainitic ferrites were formed, as shown in Figures 3(c) and (d), indicated by red arrows. This type of microstructural development is predicted to be type A, and blocky M-A is expected to form between the PAGB and bainitic ferrite observed in Figure 3(b).

Figure 4(a) shows the α -orientation map (superimposed with the image quality map) and analyzed variant pair that correspond to Figure 3. As shown in Figure 4(a), a coherent twin boundary was confirmed and type A microstructural development was observed

between the twin boundary and PAGB. When the first bainitic ferrite is assumed to be V8, the bainitic ferrite indicated by an arrow in Figure 3(c) is identified as V8. As expected, the bainitic ferrite indicated by an arrow in Figure 3(d) is identified as V1 and V4 pair. Furthermore, another V1 and V4 pair is identified within this area, which is an important condition for this bainitic ferrite to be classified as type A. It was also confirmed that there was a temperature difference between V1 and V8 formation. An image quality map superimposed with the phase map for austenite (green color) is shown in Figure 4(b). The large blocky area can be identified within this area, and it is between V1 and V8. This area contains the fine ferrite phase with high and low image quality. As described by Lambert *et al.*,^[10] a part of this blocky area contains decomposed ferrite and carbide with a small amount of M-A and austenite phases. As expected, the stability of blocky austenite formed in type A mode is low. A fraction of retained austenite is around the blocky area, as indicated by red arrows in Figure 4(b).

The bainitic ferrite indicated by a blue arrow in Figures 3(a) and (b) shows the characteristics of type B mode as expected and contains the elongated retained austenite, as shown in Figure 4(b), indicated by a blue arrow. These results indicate that the characteristics of M-A (*e.g.*, the morphology and the stability of austenite and its distribution) in the HAZ region can be predicted through the analysis of the microstructural development.

The correlation between the microstructural development of bainitic ferrite under a simulated weld HAZ and the characteristics of M-A formed was shown using LSCM observations and EBSD analysis. There were two distinct types of microstructural development, which were classified as types A and B.

In the type A development, bainitic ferrite first grew closely parallel to the PAGB at higher temperatures. As the temperature decreased, the variant pair having low-angle misorientation developed (same Bain group and different CP group) and blocky M-A (including partially decomposed ferrite and carbide) was formed at these variant boundaries. The retained austenite exhibited low

stability. In the type B development, bainitic ferrite first grew with a high angle against the PAGB. Subsequently, the single variant grew by thickening (side by side), and an elongated M-A with high stability was homogeneously distributed.

Our study provides the possibility of predicting the M-A characteristics from the observations of microstructural morphology.

This work was supported by JSPS KAKENHI Grant No. 24560879.

REFERENCES

1. J.H. Chen, Y. Kikuta, T. Araki, M. Yoneda, and Y. Matsuda: *Acta Metall. Mater.*, 1984, vol. 32, pp. 1779–88.
2. C.L. Davis and J.E. King: *Metall. Mater. Trans. A*, 1994, vol. 25A, pp. 563–73.
3. L.Y. Lan, C.L. Qiu, D.W. Zhao, X.H. Gao, and L.X. Du: *Mater. Sci. Eng. A*, 2011, vol. 529, pp. 192–200.
4. L.Y. Lan, C.L. Qiu, D.W. Zhao, X.H. Gao, and L.X. Du: *Mater. Sci. Eng. A*, 2012, vol. 558, pp. 592–601.
5. S.H. Lee, B.C. Kim, and D.G. Kwon: *Metall. Trans. A*, 1993, vol. 24A, pp. 1133–41.
6. T. Furuhashi, H. Kawata, S. Morito, and T. Maki: *Mater. Sci. Eng. A*, 2006, vol. 431, pp. 228–36.
7. T. Furuhashi, H. Kawata, S. Morito, G. Miyamoto, and T. Maki: *Metall. Mater. Trans. A*, 2008, vol. 39A, pp. 1003–13.
8. A. Lambert-Perlade, A.F. Gourgues, and A. Pineau: *Acta Mater.*, 2004, vol. 52, pp. 2337–48.
9. N. Takayama, G. Miyamoto, and T. Furuhashi: *Acta Mater.*, 2012, vol. 60, pp. 2387–96.
10. A. Lambert, J. Drillet, A.F. Gourgues, T. Sturel, and A. Pineau: *Sci. Technol. Weld. Join.*, 2000, vol. 5, pp. 168–73.
11. H. Terasaki and Y. Komizo: *Metall. Mater. Trans. A*, 2013, vol. 44A, pp. 2683–89.
12. H. Chikama, H. Shibata, T. Emi, and M. Suzuki: *Mater. T. Jim*, 1996, vol. 37, pp. 620–26.
13. S.I. Wright and M.M. Nowell: *Microsc. Microanal.*, 2006, vol. 12, pp. 72–84.
14. S. Morito, H. Tanaka, R. Konishi, T. Furuhashi, and T. Maki: *Acta Mater.*, 2003, vol. 51, pp. 1789–99.